



Energy based techno-economic and environmental feasibility study on PV/T and PV/T heat pump system with phase change material—a numerical comparative study

Prakash K. Babu¹ · Amarkarthik Arunachalam¹ · Subramaniyan Chinnasamy¹ · Chandrasekaran Manimuthu¹

Received: 22 July 2023 / Accepted: 12 January 2024 / Published online: 1 February 2024
© The Author(s), under exclusive licence to Springer-Verlag GmbH Germany, part of Springer Nature 2024

Abstract

A sustainable, affordable, and eco-friendly solution has been proposed to address water heating, electricity generation, space cooling, and photovoltaic (PV) cooling requirements in scorching climates. The photovoltaic thermal system (PV/T) and the direct expansion PV/T heat pump (PV/T DXHP) were numerically studied using MATLAB. A butterfly serpentine flow collector (BSFC) and phase change material (PCM) were assimilated in the PV system and MATLAB model was developed to evaluate the economic and enviroeconomic performance of the PV/T water system (PV/T-W), PV/T PCM water system (PV/T PCM-W), the PV/T DXHP system, and the PV/T PCM heat pump system (PV/T-PCM-DXHP). In this study, annual energy production, socioeconomic factors, enviro-economic indicators, and environmental characteristics are assessed and compared. Also, an economic, environmental, and enviro-economic analysis was conducted to assess the commercial viability of the suggested system. The PV/T PCM-DXHP demonstrated the highest electrical performance of 53.69%, which is comparatively higher than the other three configurations. The discounted levelized cost of energy (DLCOE) and payback period (DPP) of the PV/T PCM-DXHP were ₹2.87 per kW-h and 3–4 years, respectively, resulting in a total savings of ₹67,7403 over its lifetime. Furthermore, installing this system mitigated 280.72 tonnes of CO₂ emissions and saved the mitigation cost by ₹329,700 throughout its operational lifecycle.

Keywords Solar PV · PV/T · Heat pump · Energy · COP · PCM · Economic · Environmental

Introduction

Among the renewable energy (RE) sources, solar energy (SE) is a precious resource with great potential for addressing India's energy deficit. India's solar PV energy generation capacity is less than 6.5% (Rauf et al. 2023). India's primary objective in the field of energy is to give the most priority to energy conservation, energy efficiency, and the effective use of RE resources (Kaleshwarwar and Bahadure 2023). Solar energy has the ability to encounter the mounting energy demand in India (Gielen et al. 2019). India's mammoth land area receives significant SE, estimated at 5000

trillion kW-h annually. India receives a daily average solar irradiation between 4 and 7 kW-h per m² of SE (Batool et al. 2023). Solar PV offers scalability, allowing for the deployment of solar energy systems at various capacities to meet the energy requirements of India (Bhanja and Roychowdhury 2023) and it contributes to mitigating climate change. The cultivation of SE is the only option to meet the target of the Paris agreement by reducing the annual reduction of 1.5 °C in ambient temperature (Fawzy et al. 2020). Further, this system mitigates the gases CO₂, SO₂, NO_x, PM_{2.5}, and PM₁₀, which contribute to greenhouse gas emissions (Jäger-Waldau et al. 2020; Kazem et al. 2023). In addition to this pledge, India focuses on installing net zero energy in newly constructed buildings and almost energy-free buildings that get all the power they need from the sun, wind, or other RE resources. However, since solar PV productivity is so low, the practical utilization of SE in the power system is less than 10% (Dubey et al. 2013; Alharbi and Kais 2015). Therefore, hybrid PV/T-W systems have gained popularity recently because they combine the PV and solar

Responsible Editor: Philippe Garrigues

✉ Prakash K. Babu
kbprakash404@gmail.com

¹ Department of Mechanical Engineering, Bannari Amman Institute of Technology, Sathyamangalam, Erode, Tamil Nadu, India 638401

water heating systems into a single module (Emmanuel et al. 2021). The PV system converts the SE into usable electricity and heat through photovoltaic and thermal conversion (Obalanlege et al. 2020). However, because of the incorporated thermal unit, the price of PV/T-W is significantly greater than traditional PV (Abdul Jabar et al. 2023). Hence, a cost–benefit analysis is needed to figure out how beneficial these systems are in real life. Also, it is essential to identify the environmental benefits to society (Beniwal et al. 2023).

The PV/T-W systems, in particular, can breed power and hot water to the buildings (Sharaf et al. 2022). Kalogirou and Tripanagnostopoulos (2007) evaluated the PV/T-W system, proving it saved more cost than the reference uncooled PV. Herrando and Markides (2016) investigated an economic analysis of the PV/T-W, and it reduced the life cycle cost of energy (LCOE) and mitigated the CO₂ but with a higher capital cost for UK climatic conditions. Tse et al. (2016) studied an energy and economic analysis of the PV/T-W system in Hong Kong. They discovered the superiority of PV/T-W panels, which have a shorter payback period and higher performance efficiency due to using the panels' waste heat. Similarly, Canelli et al. (2015) performed a simulation in Italy on the same system and reduced 36.2% and 28.4% of CO₂ emissions and operating costs, respectively. Bianchini et al. (2017) analyzed the PV/T-W system and found that LCOE is lower than the country's energy cost. PCMs are also employed to cool the PV system, and storing the excess heat from the PV panel rose the overall efficiency, decreasing the life cycle cost and CO₂ destruction (Lamba et al. 2023). Hossain et al. (2019) conducted an experimental study in Malaysian climatic conditions on the PV/T PCM system and revealed that incorporating PCM increases thermal and electrical efficiency. The assimilation of PCM in the PV/T PCM system increased the life of the system. Cui et al. (2022) invented that a PV/T system equipped with PCM has a 6 years shorter payback period, and is more economically viable than a PV/T system. The integration of PCM in the PV/T system saved the annual cost by 15% to 20%. The absence of adequate indulgence on the practicality and benefits of PVT-W and PV/T PCM-W has hindered the commercialization of PV/T PCM and water technologies. As a result, there is a growing amount of literature on employing heat pumps as a cost-effective and ecologically sound means of augmenting the thermal output of PV/T systems (Obalanlege et al. 2020).

A hybrid PV/T HP system is additionally used for PV cooling, water heating, and space cooling. This technology lowered the PV temperature, boosting the system's power conversion efficiency, heating value, and COP (Miglioli et al. 2021). Obalanlege et al. (2020) executed a financial analysis on PV/T HP and reported that the system's payback period increases while increasing the system's cooling capacity. Obalanlege et al. (2022) steered an economic and environmental analysis

of the PV/T HP system under UK climatic conditions and reported that the recurring cost of the proposed system is low and destroys CO₂ by 610 kg annually throughout its lifetime. Zhang et al. (2014) investigated the socio-economic assessment of the IE PV/T HP system with a loop heat exchanger. They found that it is economically suitable for London's climatic conditions and environmentally most suitable for Shanghai's climatic conditions. Liu et al. (2023) have done performance analysis and found the optimum design configuration for the PV/T-DXHP system. Abbas et al. (2023) analyzed the PV/T-DXHP systems via MATLAB and reported a maximum COP of 5.68, and its payback period was 7.15 years. Most of the research was focused on the indirect expansion of hybrid PV/T HP systems (Liu et al. 2020) rather than the direct expansion of the PV/T HP system due to its lack of control in the heat load and refrigerant leakage issues (Dannemand et al. 2019, 2020).

Though many research works on PV/T-W and PV/T DXHP systems have been conducted, there is a scarcity of studies examining the energy-based economic and environmental analysis specifically for these systems using hydrated salt PCM in hot Indian climate conditions. The novelty of this current work lies in the design and development of a new thermal collector/evaporator based on a butterfly serpentine flow configuration, and incorporating hydrated salt (HS36) PCM in the PV system for PV cooling, water heating, and space cooling applications. The numerical studies were carried out by assimilating the BSF collector and HS36 PCM in the PV system and their impact on annual energy production was found using MATLAB. Furthermore, this study aims to compare the commercial viability of PV/T systems and PV/T-DXHP systems in Indian buildings, specifically focusing on energy, economic, and environmental characteristics in hot climatic regions of India. Various factors are considered in the comparison, including total electrical and thermal energy generation, discounted net present value (DNPV), discounted payback period (DPP), levelized cost of energy (DLCOE), as well as the quantities of CO₂, SO₂, NO_x, and PM₁₀ mitigated, along with cost savings. The study aims to propose an economically and environmentally feasible system for Indian climatic conditions. By examining and comparing these aspects, the study wishes to deliver valuable insights into the performance and viability of PV/T-W, PV/T-PCM-W, PV/T-DXHP, and PV/T PCM-DXHP systems, ultimately recommending a system that is economically and environmentally suitable for the specific climatic conditions found in India.

System description

The research involved in finding the annual energy generation with a designed novel thermal collector and HS 36 PCM and predicting the economic and environmental

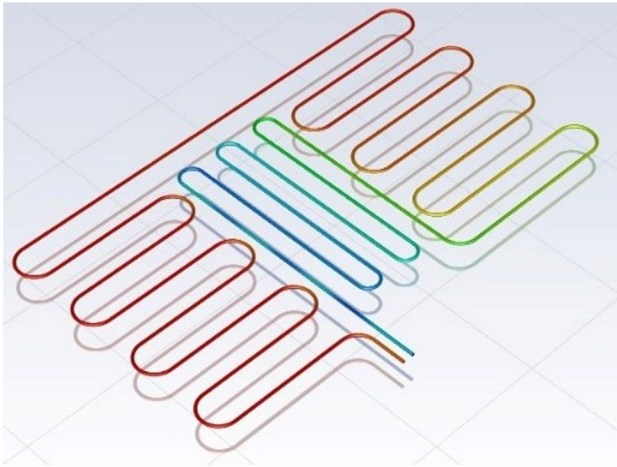


Fig. 1 Pictorial representation of Butterfly Serpentine Flow Profile

viability of the following systems. The annual energy analysis is simulated in MATLAB for the following five different configurations: PV, PV/T with water as the working fluid (PV/T-W), PV/T with phase change material (PCM) energy storage and water as the working fluid (PV/T PCM-W), PV/T with a direct expansion heat pump (PV/T DXHP), and PV/T with PCM energy storage and a direct expansion heat pump (PV/T-PCM-DXHP). Figure 1 provides a visual representation of the butterfly serpentine flow profile used in these PV/T configurations (Prakash and Amarkarthik 2023),

which was integrated into PV and made as case-1 (PV/T-W), case-2 (PV/T PCM-W), case-3 (PV/T DXHP), case-4 (PV/T-PCM-DXHP), and case-5 (uncooled PV–basic standard PV system). These system configurations are shown in Table 1.

Earlier studies have explored designs such as parallel, concentric, web spiral, bionic, and serpentine flow copper coils placed underneath PV/T panels (Poredoš et al. 2020). The butterfly serpentine flow collector (BSFC) pattern is a design that resembles the shape of a butterfly and is used in the PV/T collector. Figure 1 demonstrates the design of the PV/T collector, while Fig. 2 portrays the different layers of the PV/T and PV/T PCM collectors used for the simulations. Hydrated salt (HS36) is selected as PCM to maintain thermal stability and enhance the cooling of the PV panel. The PCM helps control the temperature of the PV panel, when the melting temperature of the PCM is around 3 °C to 6 °C higher than the ambient temperature (Waqas and Jie 2018; Velmurugan et al. 2021).

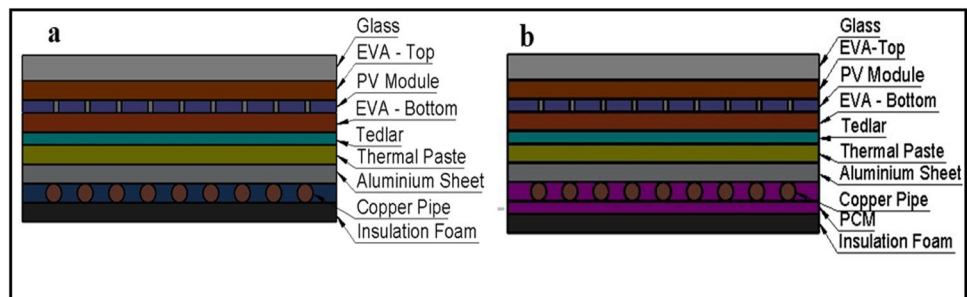
$$m_{PCM} = \frac{Q_{ch}}{Q_{LH-PCM} + \int_i^m C_{ps}(T)dT + \int_m^f C_{pl}(T)dT} \tag{1}$$

The simulation setup of the proposed system is shown in Fig. 3 a and b. In this system, solar energy is incident upon the PV/T thermal system’s panels. In the PV/T system, a water tank is a storage unit where water is pumped to the panel. This water tank acts as a reservoir to store the heat,

Table 1 Different kinds of systems used in this work

Cases	Symbols	PV	PV/T	HP	Water	R410a	PCM
Case 1	PV/T-W	✓	✓	✗	✓	✗	✗
Case 2	PV/T-PCM-W	✓	✓	✗	✓	✗	✓
Case 3	PV/T-DXHP	✓	✓	✓	✗	✓	✗
Case 4	PV/T-PCM-DXHP	✓	✓	✓	✗	✓	✓
Case 5	PV	✓	✗	✗	✗	✗	✗

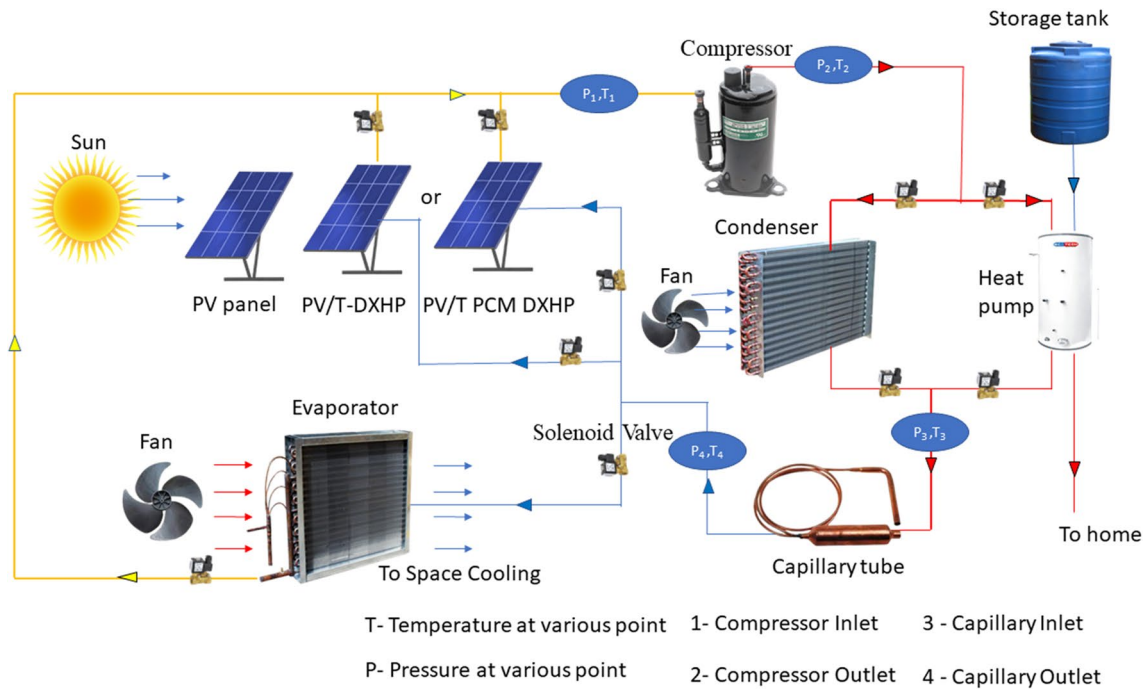
Fig. 2 Pictorial representation of layers and formation of **a** PV/T-W and **b** PV/T PCM-W



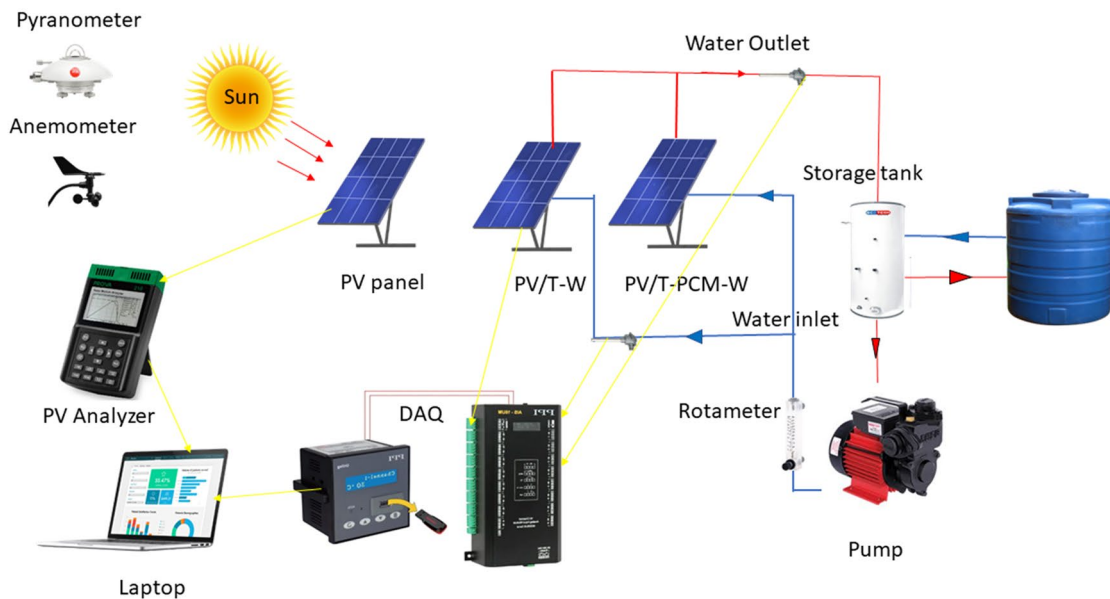
which is recovered from the system. In the PV/T DXHP system, a heat pump is employed to circulate refrigerant instead of water. The compressor extracts the refrigerant from the PV/T evaporator and increases its pressure to that of the condenser. As the refrigerant flows into the condenser tank, it transfers heat to the water in the tank. The pressure of the refrigerant significantly decreases as it passes through the expansion valve. In the meantime, the liquid refrigerant

enters the PV/T evaporator, which contributes to the PV system’s cooling by absorbing heat from the panels. Ultimately, the PV/T heat pump system cools the photovoltaic panels and heats the water.

The place chosen for the simulation study is located at the coordinates of 11.4963° N, 77.2769° E, in Sathyamangalam, Tamilnadu, India. The average temperature of this field is around 31 °C, the average wind speed is 6.5 m/h,



a



b

Fig. 3 **a** Schematic line diagram of the PV/T DXHP setup. **b** Schematic line diagram of the PV/T-W and PV/T PCM-W setup

air mass (AM) is 1.5, and the average relative humidity is 66%. The sun shines up to 5.8 h/day and the topography is close to the Western Ghats and the Bhavanisagar dam. In this study, the inclination of the PV was kept at 11.5° south. The latitude of the location chosen sets the angle (β) of the PV/T panel (Muthu and Ramadas 2023). For the numerical study, a polycrystalline PV panel with a capacity of 260 W is chosen. Table 2 highlights the panel’s most salient features of PV, PV/T, and PCMs used in this numerical work. Similarly, Table 3 provides the technical details of the heat pump used in the system.

System simulation model

For the numerical study, a polycrystalline PV panel with a capacity of 260 W is chosen. Table 2 highlights the panel’s most salient features. It is presumed that the panel functions in conditions that are consistent with a steady state. This assumption is reasonable because the temporal fluctuations of the boundary conditions are relatively slow compared to the dynamic response of the panel (Guarracino et al. 2016).

Table 2 Technical parameters of PV module and PCM

Parameters	Nomenclature	Value	Unit
PVGC thickness	δ_c	1	mm
PVGC emissivity	ϵ_c	0.84	[-]
PVGC transmissivity	τ_c	0.9	[-]
SC thickness	δ_{pv}	0.3	mm
SC emissivity	ϵ_{pv}	0.96	[-]
SC absorbance	a_{pv}	0.85	[-]
SC thermal conductivity	κ_{pv}	203	W/m.°C
Reference SC electrical efficiency	η_{std}	16.0	%
SC temperature coefficient at SSC	β_{sc}	0.031	%/°C
SC temperature coefficient at VOC	β_{oc}	-0.390	%/°C
SC temperature coefficient at FF	β_{ff}	-0.166	%/°C
Standard SC’s SSC	$I_{ref,sc}$	9.030	A
Standard SC’s VOC	$V_{ref,oc}$	0.657	V
Standard SC’s FF	FF_{ref}	0.820	[-]
No SC in the PV system	n	60	[-]
Tadlar absorbance	a_b	0.8	[-]
EVAG thickness	δ_{EVA}	0.5	mm
EVAG thermal conductivity	κ_{EVA}	0.311	W/m.°C
Packing factor	β_{pv}	0.9	[-]
PV/T module area	A	1.66	m ²
Aluminium sheet thickness	δ_{rb}	0.8	mm
Refrigerant type	ref	R410a	[-]
Melting point	T_m	°C	36.0
Freezing point	T_{fz}	°C	35.0
Latent heat	Q_{LH-pcm}	kJ/kg	166

Table 3 Parametric description of the DXHP system

Materials	Factor	Values
R410 a compressor	Power supply	220/240 V–50 Hz–1 Ph
	Volume (displacement)	10.8 (cc/rev)
	Input power (rated)	910 W
	Current (rated)	4 A
	Heating capacity	3500 W
	Refrigerant	R410a
Capillary tube	Diameter	1.5 mm
	Length	50 mm
Condenser	Coil diameter	¼ in
	Coil OD	9.52 mm
	Coil ID	7.75 mm
	Tank capacity	500 L
	Coil length	20 m
Air source evaporator	Coil OD	9.52 mm
	Coil ID	7.75 mm
	Fin pitch	9.5 mm
	Tube pitch	20 mm

PV/T system model

Equations (2), (3), (4), (5), (6), (7), (8), and (9) express the glass cover model, PV model, heat absorber, Piping model, bonding model, working fluid model, insulation model, aluminium plate models (Obalanlege et al. 2022), and PCM models (Yang et al. 2019).

$$G\alpha_g = (h_{v,g-a} + h_{ra,g-s})(T_g - T_a) + h_{d,g-pv}(T_g - T_{pv}) \quad (2)$$

$$I\tau_g\alpha_{pv} [1 - PA\eta_{tra}(1 - \beta(T_{pv} - T_a))] = h_{d,g-pv}(T_{pv} - T_g) + h_{d,pv-abs}(T_{pv} - T_{abs}) \quad (3)$$

$$h_{d,pv-abs}(T_{pv} - T_{abs}) = h_{d,abs-t}(T_{abs} - T_t) + h_{d,abs-ig}(T_{abs} - T_{ig}) \quad (4)$$

$$h_{d,abs-t}(T_{abs} - T_t) = h_{v,t-w}(T_t - \bar{T}_w) + h_{d,t-ig}(T_t - T_{ig}) \quad (5)$$

$$h_{v,t-w}(T_t - \bar{T}_w)A = \dot{m}_{w,pvt}c_p(T_{w,out} - T_{w,in}) \quad (6)$$

$$h_{d,abs-ig}(T_{abs} - T_{ig}) + h_{d,t-ig}(T_t - T_{ig}) = h_{d,ig-ip}(T_{ig} - T_{ip}) \quad (7)$$

$$h_{d,ip-al}(T_{ip} - T_{al}) = h_{v,al-a}(T_{al} - T_a) \quad (8)$$

$$\rho_{g-pcm} = \rho_{pcm} [1 - B_{pcm}(T_{pcm} - T_{ref})] \quad (9)$$

Equations (2), (3), (4), (5), (6), (7), and (8) are given as model equations in MATLAB and simulated by the procedure shown in Fig. 4 a. The temperature of the PV module and the inlet and outlet temperatures of the water were found. Equation (10) was used to get the electrical efficiency (η_{el}) of a 260-W photovoltaic panel, and Eq. (11) was used to determine the thermal efficiency (η_{th}) of the PV/T system. Finally, Eqs. (12), (13), and (14) (Yang et al. 2019) were used to calculate the total heat and electrical power generated throughout the year using simulated data from MATLAB. The combined energy produced from the PV/T systems was calculated using Eqs. (12), (13), and (14) (Gu et al. 2018).

$$\eta_{el} = \eta_{ref} [1 - \beta(T_{PV} - T_{ref})] \tag{10}$$

$$\eta_{th} = \frac{\dot{m}_{w,pvt} c_p (T_{out} - T_{in})}{G \cdot A} \tag{11}$$

$$E_{pvt,t} = E_{dc,t} + E_{th,t}, \tag{12}$$

$$E_{dc,t} = (D_t \times G_t \times \eta_{dc} \times A_{dc})(1 - dg)^{t-1} \tag{13}$$

$$E_{th,t} = (D_t \times G_t \times \eta_{th} \times A_{th})(1 - dg)^{t-1} \tag{14}$$

PV/T DXHP system model

Using MATLAB, the following Eqs. (15)–(24) used to simulate the PV/T DXHP system and its simulation procedure are shown as a flow chart in Fig. 4 b. Equations (15)–(17) are the energy balance equations used to model the compressor (Obalanlege et al. 2022).

$$\dot{m}_{k,r} = \omega_k V_k \rho_{k,r} \eta_k \tag{15}$$

$$\rho_{k,r} = f(P_{k,r}, h_{k,r}) \tag{16}$$

Equation (17) represents the condenser model (Zhou et al. 2019), which is derived based on enthalpy change in refrigerants.

$$Q_{cond} = m_{ref} (h'_{Con,out} - h'_{Con,in}) = m_w C p_w (T_o - T_i) \tag{17}$$

Equations (18)–(21) show the solar PV/T evaporator models (Deng and Yu 2016). Equation (22) shows the expansion valve model.

$$Q_e = A_{cl} [\alpha I_T - U_{Lc} (T_{PV} - T_a)] = F t A_{cl} [\alpha I_T - U_{Lc} (T_{fm} - T_a)] \tag{18}$$

$$U_{Lc} = h_v + h_r, \tag{19}$$

$$h_v = 2.8 + 3u_w \tag{20}$$

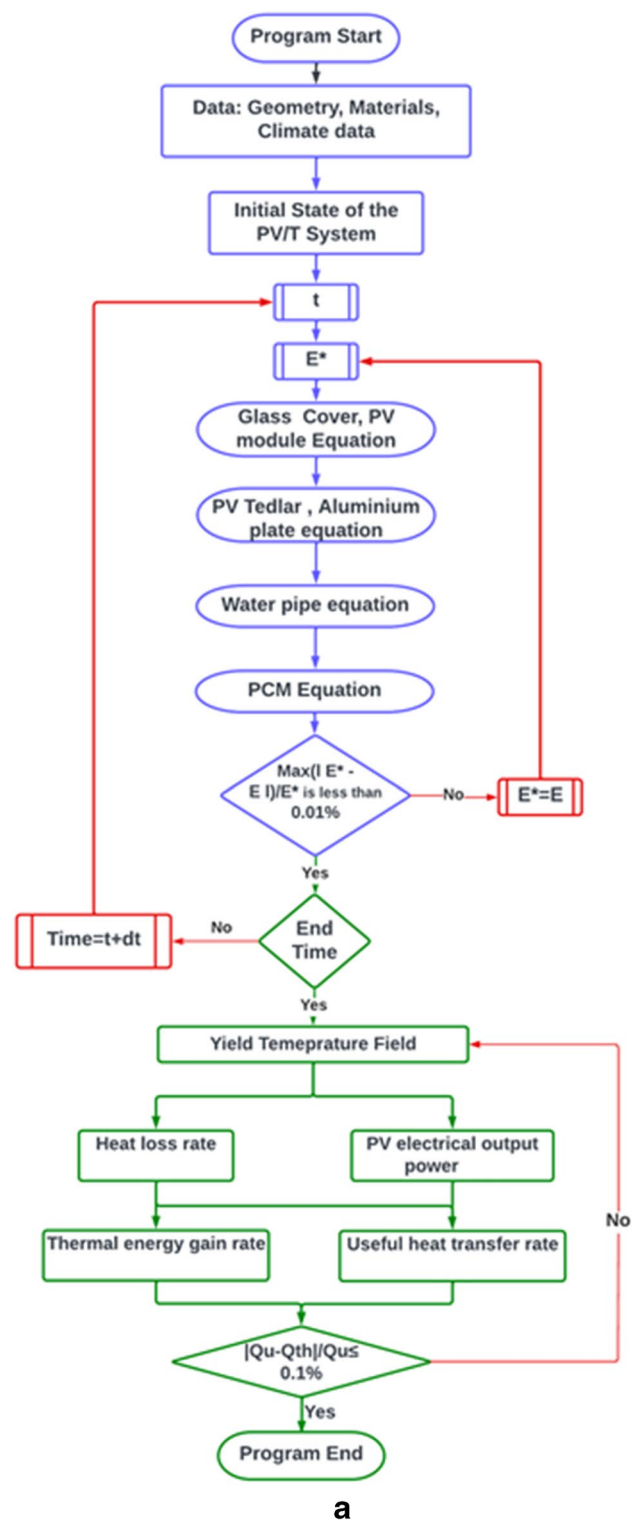


Fig. 4 a Flowchart of simulation methodology of case 2 system. **b** Simulation methodology of case 3 system

$$h_r = \epsilon \sigma (T_p^2 + T_a^2) (T_p + T_a) \tag{21}$$

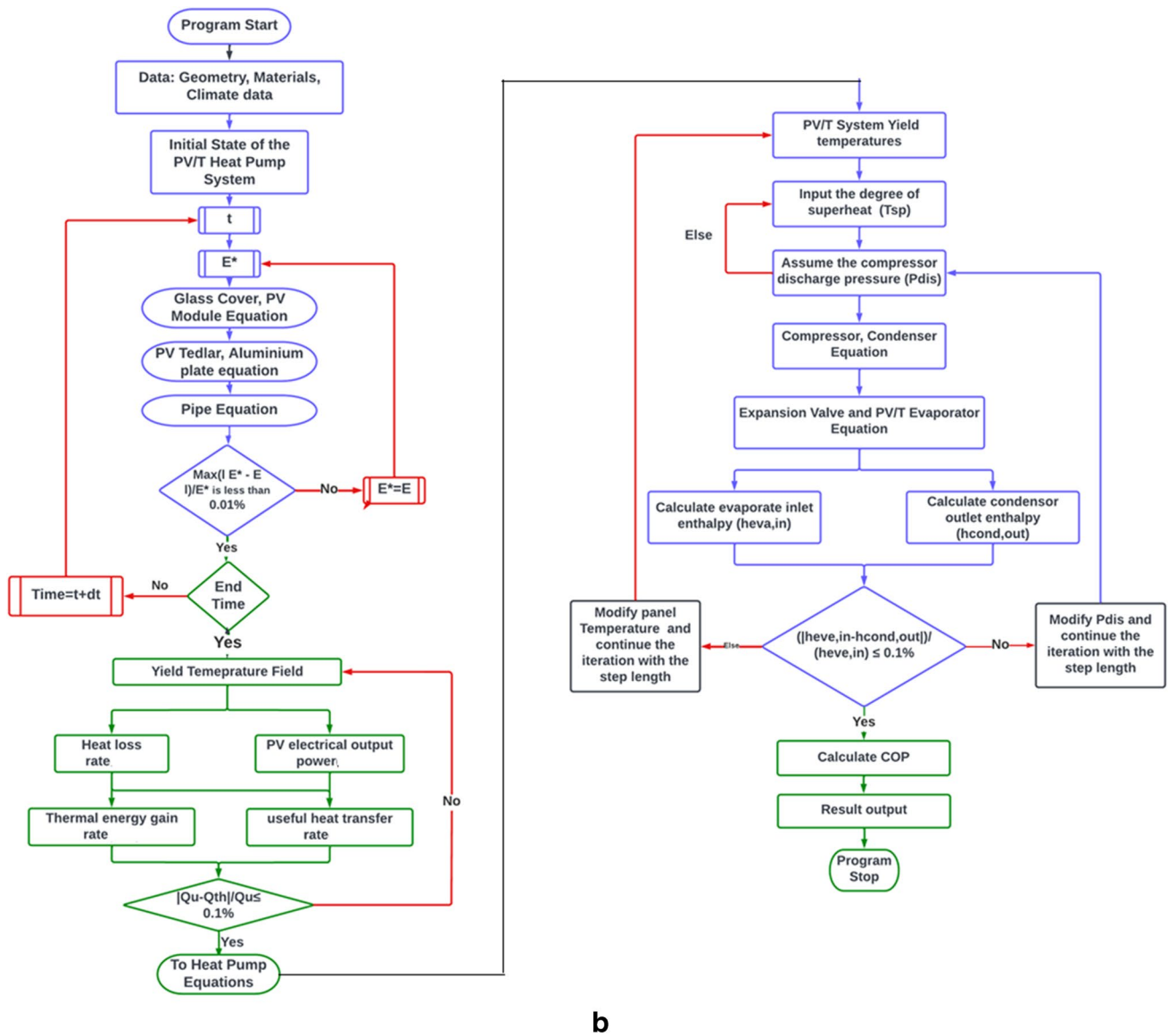


Fig. 4 (continued)

$$h_{c,r} = h_{e,r} \tag{22}$$

Equation (23) mentions the thermal efficiency (η_{thHP}) of the PV/T HP system (Lu et al. 2019).

$$\eta_{thHP} = \frac{Q_{cond} - P_{com}}{A * G} \tag{23}$$

Economic model

The techno-economic evaluation inside this work divides the system’s initial cost of investment and implementation expenses (Ehyaei et al. 2019). The system’s initial investment cost is divided further into expenses for the components used

and their corresponding installation charges. These prices were received from the dealer as quotes. Table 4 shows the pricing and suppliers. The system’s operational and servicing costs are included in the yearly expenses. The total combined cost (TCC) is the summation of all the costs a system has incurred over its lifetime. It is expressed in Eq. (24) (Coffey et al. 2016). The annual cash flow (ACF) analysis is an excellent way to compute the annual economic result of the case 1 and 2 systems with the impact of discount rates (r) and inflation rates (i). Discounted net present value (DNPV) calculates the current value of an investment by taking into account its overall value during its whole duration and adjusting for the time value of money. It is calculated using Eqs. (25) and (26) (Herbohn et al. 2002). The discounted payback period (DPP) indicates the

duration required for an investment to recoup its initial expenditure while considering the impact of the time value of money (Bhandari 2009; Rappaport 1965). Similarly, leveled cost of energy (LCOE) replicates the lifecycle expense of the system per unit of electricity produced (Obalanlege et al. 2022), which are expressed using Eqs. (27)–(29). All the equations of economic and environmental models were given as input model to MATLAB and results were found.

$$TCC_n = C_0 + C_{grid} + \sum_{n=1}^{iL} C_{O\&M} \tag{24}$$

$$ACF = \sum_{n=1}^{iL} CF_n * \frac{(1+i)^n}{(1+r)^n} \tag{25}$$

$$DNPV = -C_0 + \sum_{n=1}^{iL} CF_n * \frac{(1+i)^n}{(1+r)^n} \tag{26}$$

$$DPP = \frac{\ln\left[\frac{C_0(i-r)}{C_s} + 1\right]}{\ln\left[\frac{1+i}{1+r}\right]} \tag{27}$$

$$C_s = E_{produced} + Q_{produced} - C_{O\&M} \tag{28}$$

$$LCOE = \frac{C_0 + \sum_{n=1}^{iL} C_{O\&M} * (1+i)^{i-1} (1+r)^{-i}}{\sum_{n=1}^{iL} (E_{produced} + Q_{produced}) (1+r)^{-i}} \tag{29}$$

Environmental model

It is crucial to assess and compare the carbon emissions over the lifespan of power production systems that pose risks to public health to determine the level of tolerance for each cases. With aid of Eqs. (32) and (33), the annual CO₂ reduction and cost saving by mitigation of the proposed systems are calculated (Tiwari et al. 2015). The worldwide

Table 5 The details of the intensity and cost of pollutant mitigation (den Elzen et al. 2011; Caliskan et al. 2012)

Components	Average equivalent intensity for standard coal	Mitigation cost
CO ₂	2.493 kg/kg	1200 ₹/ton
SO ₂	0.075 kg/kg	7500 ₹/ton
NO _x	0.0375 kg/kg	45,000 ₹/ton
PM ₁₀	5.40 g/kg	52,000 ₹/ton

carbon price ranges between 13 and 16 dollars per tonne of CO₂. As a result, the mean values of 14.5 \$/t CO₂ are used to calculate the environmental cost, provided in Eq. (33) (Rajoria et al. 2013). Similarly, SO₂ mitigation (ϕ_{SO_2}), NO_x mitigation (ϕ_{NO_x}), and particulate matter ($\phi_{PM_{10}}$) mitigation and cost savings for this reduction are also calculated using Eqs. (32) and (33) (Amoatey et al. 2019). Table 5 shows the details of the intensity and cost of pollutant mitigation.

$$\phi_{CO_2} = \frac{\Psi_{CO_2} * E_{overall}}{1000} \tag{32}$$

$$Z_{CO_2} = Y_{CO_2} * \phi_{CO_2} \tag{33}$$

Validation of model

The RMSD (root mean square deviation) approach is used to prove that the findings of the simulation with the experimental observations are merely identical (Guo et al. 2015):

$$RMSD = \sqrt{\frac{1}{n} \sum_{i=1}^n [(X_{sim,i} - X_{exp,i}) / X_{exp,i}]^2} \tag{34}$$

Validation of result

With the help of MATLAB, simulation results were developed, and the results were compared with the actual data obtained in real-time experimentation. The detailed

Table 4 Price and supplier details of the components

Component name	Price in INR	Supplier
PV panel	9000	Olitec, Tamilnadu
Copper coil	3500	Sri Golden Refrigeration, Tamilnadu
PCM-HS36	6000	PLUSS, Haryana
Thermal paste	1000	PIDITHERM
Rotameter	1500	Amazon
Pump and heat pump set up	40,000	Mechzhaphire Engineering solutions
Solenoid valves	16,000	Rishab Enterprises, Tamilnadu
Refrigerant	1200	Sri Golden Refrigeration, Tamilnadu
Insulation materials	1000	Sri Golden Refrigeration, Tamilnadu
Fabrication cost	6000	-

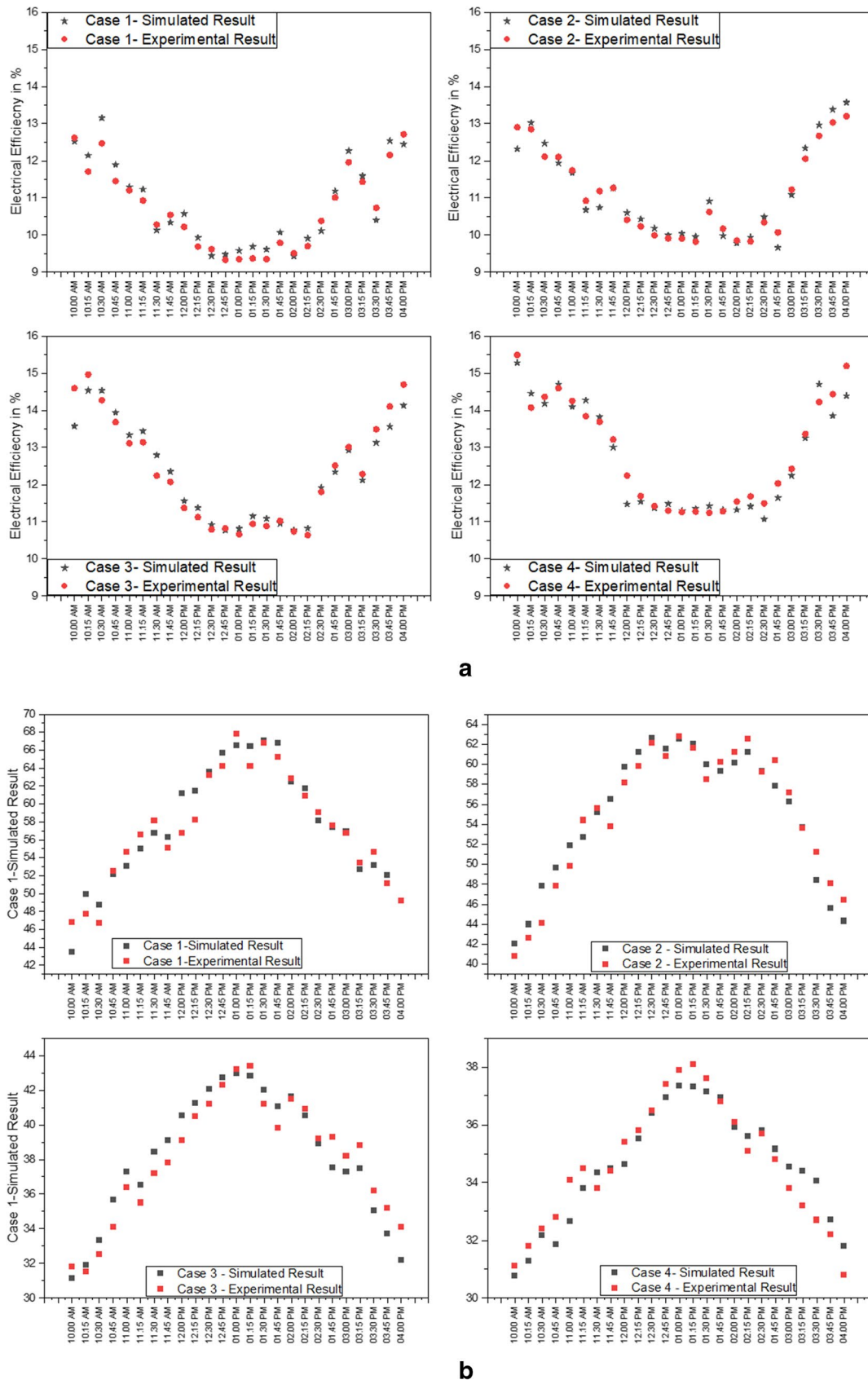
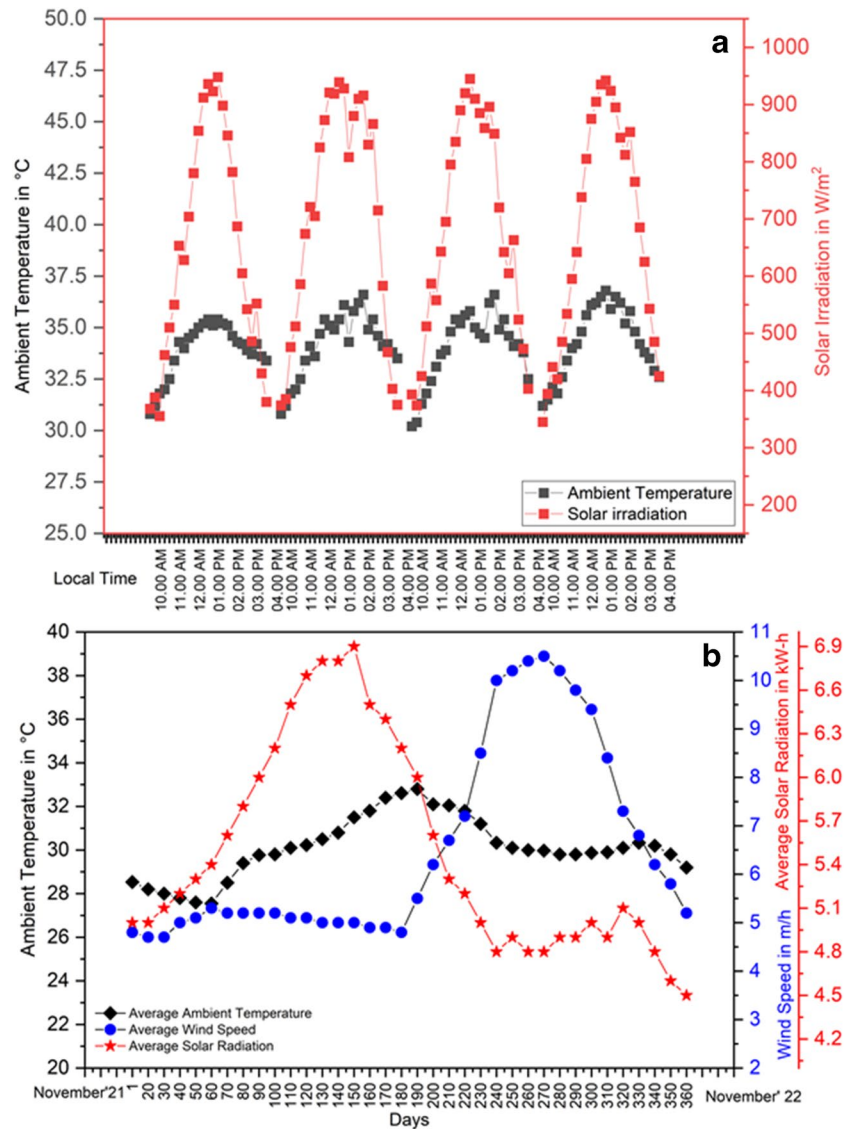


Fig. 5 a Validation of η_{el} between simulated and experimental values. b Validation of T_{PV} between simulated and experimental values

Fig. 6 Ambient conditions of chosen location for simulation study: **a** day; **b** year



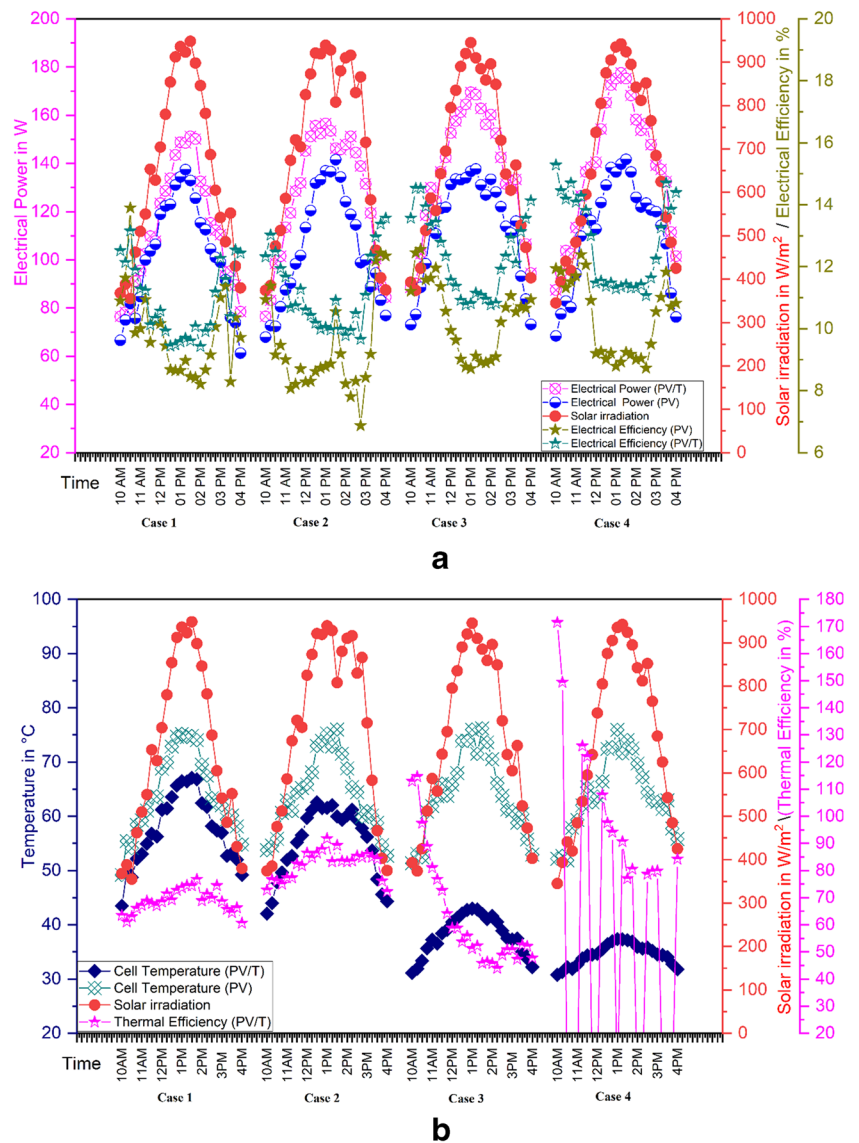
experimentation is explained in the author's previous article (Prakash and Amarkarthik 2023). The comparative analysis of the experimental data and the simulation data of electrical efficiency is depicted in Fig. 5 a, for case 1, 2, 3, and 4 systems. The values of RMSD for the η_{el} of the case 1, 2, 3, and 4 systems were 2.66%, 2.25%, 2.54, and 2.56%, respectively. Similarly, Fig. 5 b compares the T_{PV} of simulation and experimental results for all four systems. The RMSD values of PV/T cell temperature for case 1, 2, 3, and 4 systems were 2.60%, 3.25%, 2.78%, and 2.06%, respectively. Therefore, the efficiency and cell temperature found in the simulation are close to the efficiency found in the experiment. Hence, it is proved that the results obtained through simulations are valid. This variation could be the consequence of experimental error, which would include

errors caused by the instruments as well as the impact of the environment on the testing.

Result and discussion

This investigation used two working fluids for the case 1 and 3 systems: water and refrigerant R410a. The default time step for the iteration computation was set to 150 s. This choice was made because although a shorter time interval would improve accuracy slightly, it would significantly increase the computational workload without providing substantial benefits. The iteration process terminated when the final water temperature reached 60 °C, serving as the criterion for completion. The numerical analysis was

Fig. 7 a Numerical comparison of hourly variation of P_{max} and η_{el} of all cases. **b** Numerical comparison of hourly variation of T_{PV} and η_{th} of all cases



conducted in MATLAB, and the energy analyses covered a year-long period from November, 2021, to October, 2022, in a hot climatic region. The weather station present in the study location was used as weather data for this numerical study. Figure 6 presents the environmental characteristics for the entire year, including the average daily solar irradiation per month, monthly average wind speed, and monthly ambient temperature.

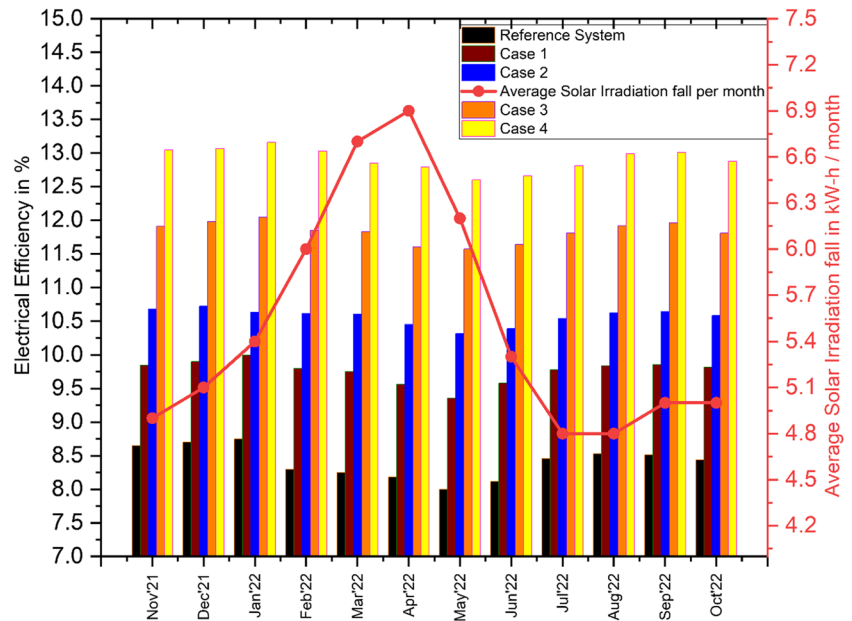
The flow of the subsequent sections is as follows: The simulation results for electrical efficiency and its average values throughout the year were discussed first. Based on these values, the total electrical power generated over the year is determined. Then, a thermal performance analysis is conducted, simulating the monthly average thermal efficiency and calculating the average total heat energy generation over the year. The combined electrical and thermal outputs are then used to evaluate the economic

and environmental performance of the case 1, 2, 3, and 4 systems.

Simulations on case 1, 2, 3, 4, and 5 systems

Simulation on case 1, 2, 3, 4, and 5 systems were done in MATLAB for a day and discussed in this section. Figure 7 a depicts the comparative simulation results of P_{max} and η_{el} of case 1, 2, 3, and 4 with the case 5 system. The average power productions of cases 1, 2, 3, and 4 were 10.51%, 20.93%, 30.74%, and 35.88% higher than the case 5 system. Similarly, the average electrical efficiencies were 10.45%, 20.40%, 29.20%, and 33.99% higher than the case 5 system. Figure 7 b illustrates the variation of T_{PV} , COP, and η_{th} of the all four systems. The average T_{PV} of case 1, 2, 3, and 4 systems were 57.50 °C, 52.98 °C, 38.12 °C, and 34.54 °C, which are 10.51%, 22.13%, 40.53%, and 45.95% lower than

Fig. 8 Graphical representation of monthly average η_{el} of all systems



the case 5 system. The average maximum η_{th} of case 1, 2, 3, and 4 systems were 76.76%, 91.75%, 114.62%, and 162.06%, respectively. Cases 3 and 4 had the highest COPs of 4.03 and 4.96, respectively. The power consumptions by cases 3 and 4 were 4.26 kWh and 3.38 kWh, respectively.

Annual electrical energy analysis

Figure 8 illustrates the simulated monthly electrical efficiency (η_{el}) results for case 1, 2, 3, and 4 systems. The electrical efficiency of these systems fluctuated with the G and reached its peak in April, 2022. Although the solar intensity in April was slightly higher than that in May and June, the average outdoor temperature in April was lower. As a result, the conversion efficiency of electrical energy was higher in April compared to May and June, but lower than in March due to the lower ambient temperature in March. Moreover, the solar intensity was lower in June and July due to cloudier and wetter days compared to April and May, resulting in decreased electricity generated during those months. The η_{el} of case 1, 2, 3, and 4 systems was higher in the winter and monsoon seasons compared to the summer, primarily due to the lower ambient temperature during those periods. However, the difference in η_{el} among all cases was relatively small during the winter and monsoon seasons. Consequently, the average η_{el} of case 1, 2, 3, and 4 systems were 16.03%, 25.53%, 40.49%, and 53.32% higher, respectively. The average yearly η_{el} of case 1, 2, 3, and 4 systems were 9.77%, 10.57%, 11.83%, and 12.91%, respectively, while it was only 8.42% for the case 5 system. The percentage of rise in η_{el} is high due to the effective cooling of PV cells due to the

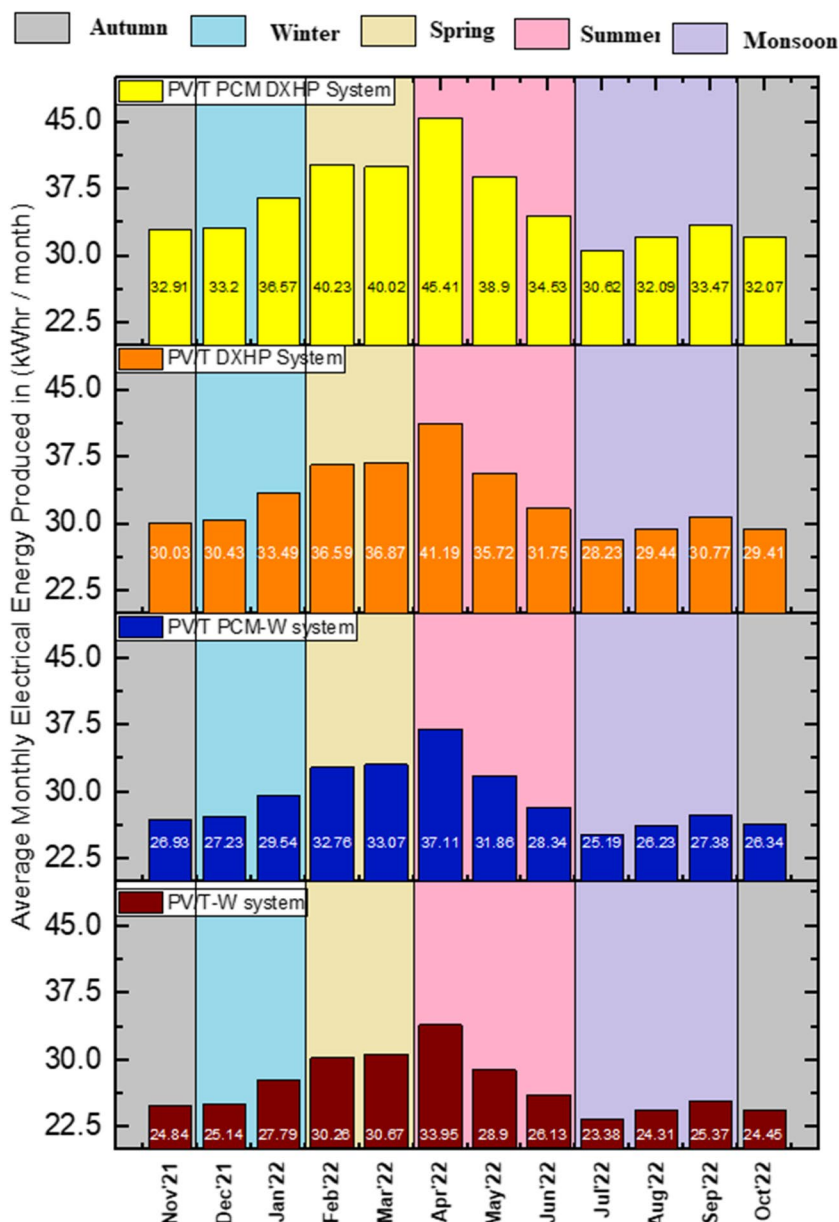
usage of cooling medium, i.e., water, PCM, and refrigerant. Therefore, Fig. 8 displays a greater degree of diversity across the different scenarios in terms of η_{el} .

The monthly electrical energy production of different systems is depicted in Fig. 9 a–d. In April, case 1, 2, 3, and 4 systems generated the highest amounts of electrical energy, 33.95 kW-h/month, 37.11 kW-h/month, 41.19 kW-h/month, and 45.41 kW-h/month, respectively. The case 5 system produced 29.4 kW-h/month during the same period. Similarly, in July, the energy production was 23.38 kW-h/month, 25.19 kW-h/month, 28.23 kW-h/month, and 30.62 kW-h/month for case 1, 2, 3, and 4 systems, with 19.98 kW-h/month in June. July experienced cloudy and muggy conditions, resulting in lower radiation and consequently reduced electrical energy generation. Comparatively, the average electrical energy productions of case 1, 2, 3, and 4 systems were 16.03%, 25.53%, 40.49%, and 53.32% higher than case 5. The total electrical energies generated per year by case 1, 2, 3, and 4 systems were 325.18 kW-h/year (1170.4 MJ), 351.98 kW-h/year (1267.13 MJ), 393.92 kW-h/year (1418.11 MJ), and 430.02 kW-h/year (1548.07 MJ), respectively. Based on these findings, the case 4 system surpasses the other three systems in power generation due to incorporating two cooling sources, namely, PCM and refrigerant. Consequently, the case 4 system offers enhanced cooling for the PV panel, leading to increased power generation.

Annual thermal energy analysis

Figure 10 provides information on the monthly average thermal efficiency (η_{th}) of case 1, 2, 3, and 4 systems. During

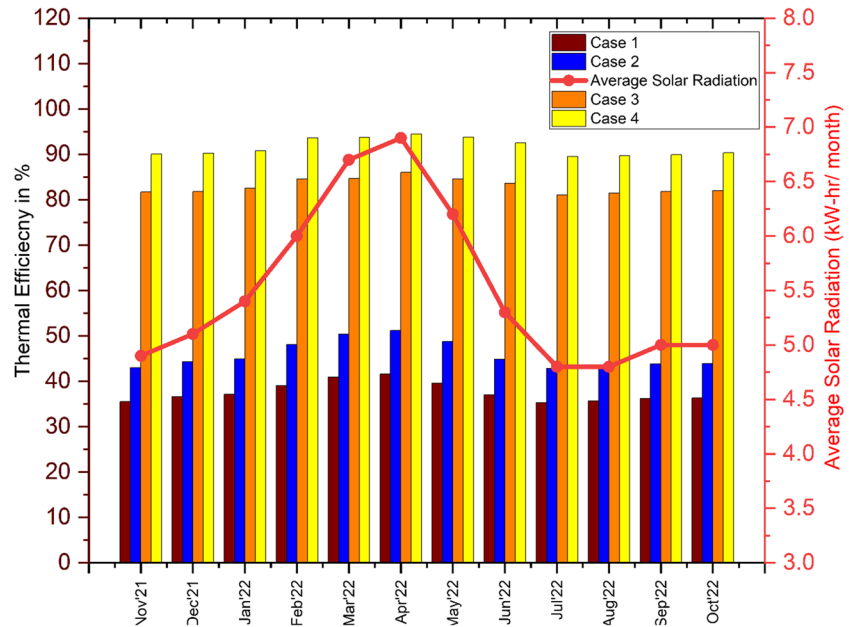
Fig. 9 Monthly average electrical energy generation



April, the highest monthly average η_{th} values were achieved, namely, 41.61%, 51.2%, 86%, and 94.54% for cases 1, 2, 3, and 4, respectively. Conversely, the lowest monthly average η_{th} values of 35.32%, 42.84%, 81.1%, and 89.5% were recorded for cases 1, 2, 3, and 4, respectively, in July. It is noteworthy that the highest thermal energies were obtained during the spring and summer seasons due to the greater solar radiation. In contrast, the lowest thermal energies were observed during the winter and monsoon seasons due to reduced solar radiation. Figure 11 displays the monthly average thermal energy produced by case 1, case 2, case 3, and case 4 systems. In April, the maximum thermal energy outputs were

531.9 MJ, 654.52 MJ, 1099.3 MJ, and 1207.9 MJ for cases 1, 2, 3, and 4, respectively, while in July, the corresponding values were 303.95 MJ, 368.76 MJ, 697.7 MJ, and 770.18 MJ. Throughout the entire year, case 1, 2, 3, and 4 systems generated 4538.66 MJ, 5534.03 MJ, 9981.07 MJ, and 11010.17 MJ of heat, respectively. Figure 12 provides an overview of the combined annual energy (electrical and thermal energy) produced by case 1, 2, 3, and 4 systems. The total energies generated by these systems, in terms of electrical and thermal energy, were 5709.35 MJ (1585.9 kW-h), 6801.16 MJ (1889.21 kW-h), 12,299.18 MJ (3416.4 kW-h), and 13,638.24 MJ (3788.4 kW-h), respectively.

Fig. 10 Monthly average thermal efficiency of all systems



Economic analysis

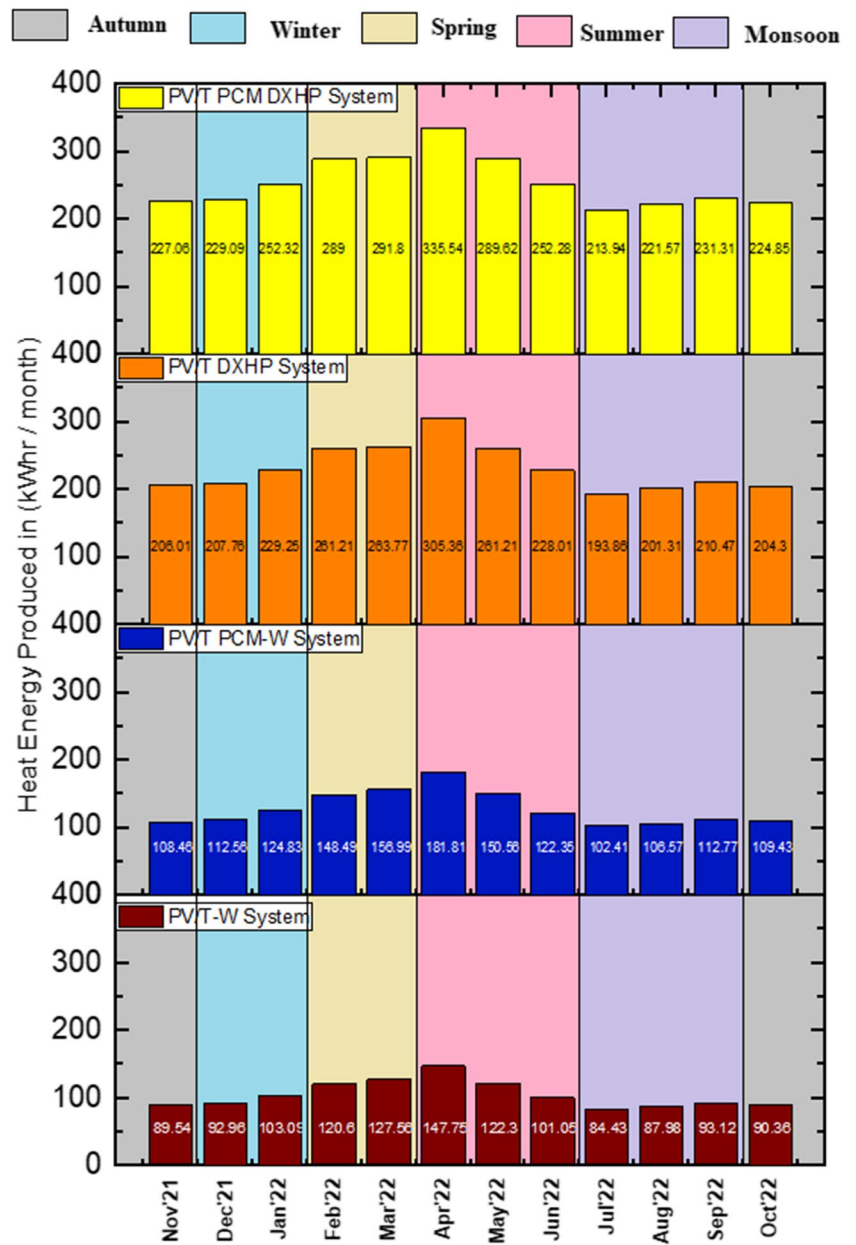
The financial analyses of case 1, case 2, case 3, and case 4 systems provide valuable insights into their feasibility in Indian climatic conditions. To assess their financial viability, the discount rate of 5.5% and the inflation rate of 6.15% were utilized for various calculations, including discounted cash flow analysis (DCFA), discounted net present value (DNPV), discounted payback period (DPBP), discounted annual cost savings (DACS), and discounted levelized cost of energy (DLCOE). This section presents these metrics, focusing on comparing all four systems with the case 5 system. In India, people are using solar water heaters, solar PV systems, and HVAC systems for water heating, electricity generation, and space cooling purposes, respectively, as individual systems. Each system has its own disadvantages. Hence, to solve its limitations and to avoid the usage of different systems, hybrid systems were proposed and the economic and environmental viability of these systems for non HVAC building and HVAC building applications is evaluated and presented. In this work, the hybrid system is designed for 1 kW electricity generation per hour and 1 tons refrigeration system with 500 L hot water capacity. In India, the average rates of 1 kW PV system, solar water heater, and air conditioner cost are ₹70,000, ₹20,000 and ₹35,000, respectively.

Figure 13 presents the annual cash flow analysis for 25 years for case 1, 2, 3, 4, and 5 systems. The average yearly cash flows for cases 1, 2, 3, and 4 are ₹4323, ₹5335, ₹15,523, and ₹22,022, respectively, and their expected payback times are 5–6, 6–7, 4–5, and 3–4 years, respectively. Figure 14 illustrates the discounted net present values (DNPV) of cases 1, 2, 3, and 4 systems, all of which have positive values.

Therefore, the installation of these systems yields a profit of ₹110,449, ₹140,083, ₹454,570, and ₹677,403, respectively, over their lifetime. The discounted payback periods (DPBPs) for cases 1, 2, 3, and 4 are 9–10, 8–9, 5–6, and 3–4 years, respectively. Moving to Fig. 15, it displays the discounted annual cost savings (DACS) and the discounted levelized cost of energy (DLCOE) for cases 1, 2, 3, and 4 systems. The DLCOE values for these systems are ₹2.92 per kWh, ₹2.78 per kWh, ₹2.34 per kWh, and ₹1.79 per kWh, respectively, whereas the DLCOE for the case 5 system without water heating cost is ₹3.62 per kW-hr. Cases 1, 2, 3, and 4 have lower DLCOE values than the reference PV system, with higher operational and maintenance costs and additional water and refrigerant pumping power. The DLCOE of the systems in cases 1, 2, 3, and 4 were lower, and likewise, the DLCOE is lower, even though all the systems have higher operational and maintenance costs and additional water and refrigerant pumping power. It is worth noting that the DLCOE values for all systems fall within the range provided by the International Renewable Energy Agency (IRENA) for residential PV installations in 2019 (₹5.25 to ₹22 per kW-h). Additionally, the DACS per year for case 1, 2, 3, and 4 systems are ₹4418, ₹5603, ₹18,183, and ₹27,096, respectively, resulting in savings of ₹110,449, ₹140,083, ₹454,570, and ₹677,403, respectively, over their lifetime. Furthermore, compared to the cost of the case 5 system, cases 1, 2, 3, and 4 saved 8.97%, 11.64%, 40.05%, and 60.16% times yielded the higher cost, respectively.

Taking into account the discounted costs and the smaller size of the reference PV system, it can be inferred that its payback period will be longer. However, considering the DPB, case 1, 2, 3, and 4 systems become profitable after

Fig. 11 Monthly average thermal energy generation by cases 1, 2, 3, and 4 systems



9–10, 8–9, 5–6, and 3–4 years, respectively. Additionally, the Indian government offers a 20% subsidy for renewable energy system installations, which further reduces the pay-back period. Consequently, the DLCOE values are lower for all the four cases when considering the water heating cost. Despite this, the DLCOE for all four systems is lower than India’s average energy cost of ₹6.15 per kW-h. Moreover, the DNPV and DACS parameters demonstrate favorable outcomes compared to the case 5 system. Furthermore, the cell temperatures of case 1, 2, 3, and 4 systems are lower than that of the case 5 system, indicating that their lifespan will likely exceed 25 years. Consequently, it is found that all the proposed systems are economically viable.

Environmental analysis

This section summarizes the annual pollution mitigation and cost savings achieved by all four systems. Figure 16a depicts the CO₂ emission mitigation and cost savings, where these four systems collectively eliminate 71.28 tons, 89.98 tons, 202.69 tons, and 280.72 tons of carbon dioxide, resulting in total cost savings of ₹83,725, ₹105,675, ₹238,050, and ₹329,700 over their lifetimes. The CO₂ mitigation and cost savings of case 1, 2, 3, and 4 systems are 3.41, 4.30, 9.68, and 13.42 times greater than case 5 system, which mitigates 20.93 tons of CO₂ and saves a total cost of ₹24,575 throughout its lifespan.

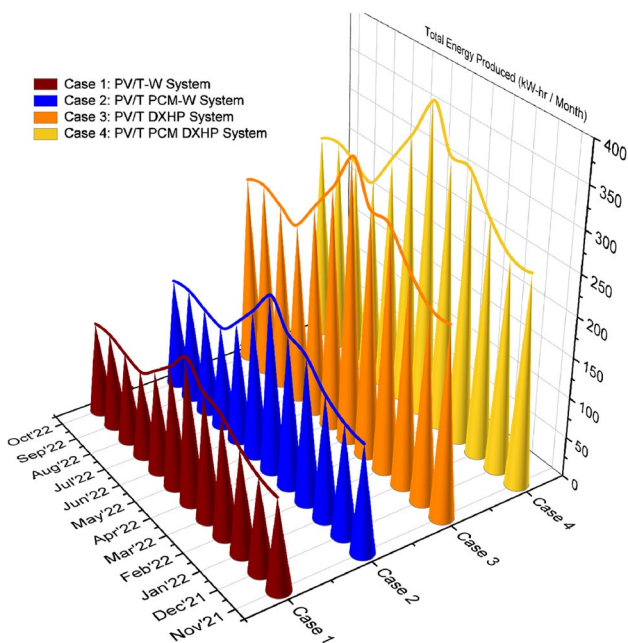


Fig. 12 Total energy generation by cases 1, 2, 3, 4, and 5 systems

Figure 16 b demonstrates the SO₂ emission mitigation and cost savings achieved by reducing pollutants. Over their lifetimes, cases 1, 2, 3, and 4 systems eliminate 2.14 tons,

2.71 tons, 6.1 tons, and 8.45 tons of SO₂, resulting in total cost savings of ₹26,050, ₹32,900, ₹74,100, and ₹102,600, respectively. The SO₂ mitigation and cost savings of case 1, 2, 3, and 4 systems are 3.41, 4.30, 9.68, and 13.42 times higher than those of the case 5 system, which mitigates 0.63 tons of SO₂ and saves a total cost of ₹7650 throughout its lifespan.

Figure 16 c focuses on reducing NO_x emissions and the associated cost savings achieved by case 1, 2, 3, and 4 systems. These systems collectively mitigate 1.07 tons, 1.35 tons, 3.05 tons, and 4.22 tons of NO_x, resulting in cost savings of ₹477,700, ₹603,000, ₹1,358,275, and ₹1,881,175, respectively, over their lifetimes. Furthermore, case 1, 2, 3, and 4 systems mitigate NO_x by 3.45, 3.49, 9.84, and 13.61 times higher than the standard PV system, which mitigates 0.31 tons of NO_x and saves a total cost of ₹140,250 throughout its lifespan.

Finally, Fig. 16 d illustrates the reduction of PM₁₀ emissions and associated cost savings achieved by case 1, 2, 3, and 4 systems. These systems mitigate 154.41 kg, 194.91 kg, 439.04 kg, and 608.05 kg of PM₁₀ emissions, resulting in cost savings of ₹93,800, ₹118,400, ₹266,725, and ₹369,400, respectively. Case 1, 2, 3, and 4 systems mitigate PM₁₀ emissions by 3.41, 4.30, 9.69, and 13.41 times higher than the standard PV system, which mitigates 45.33 kg of PM₁₀ and saves a total cost of ₹27,550 throughout its lifespan.

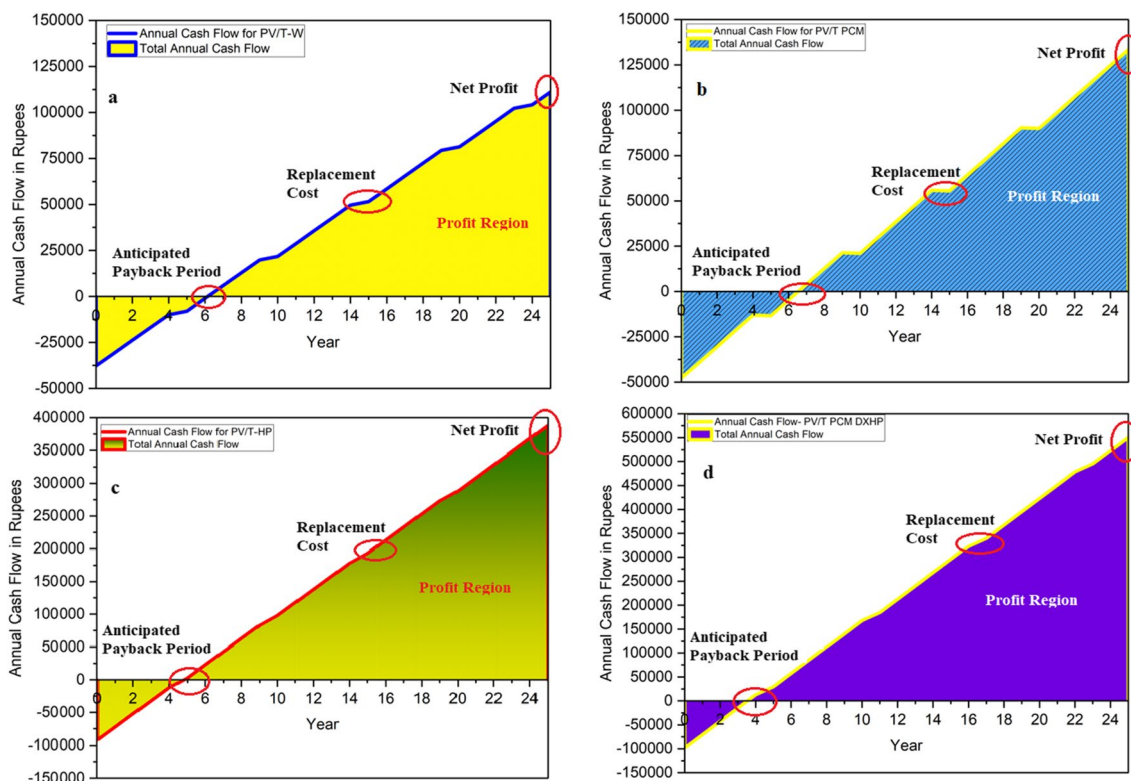
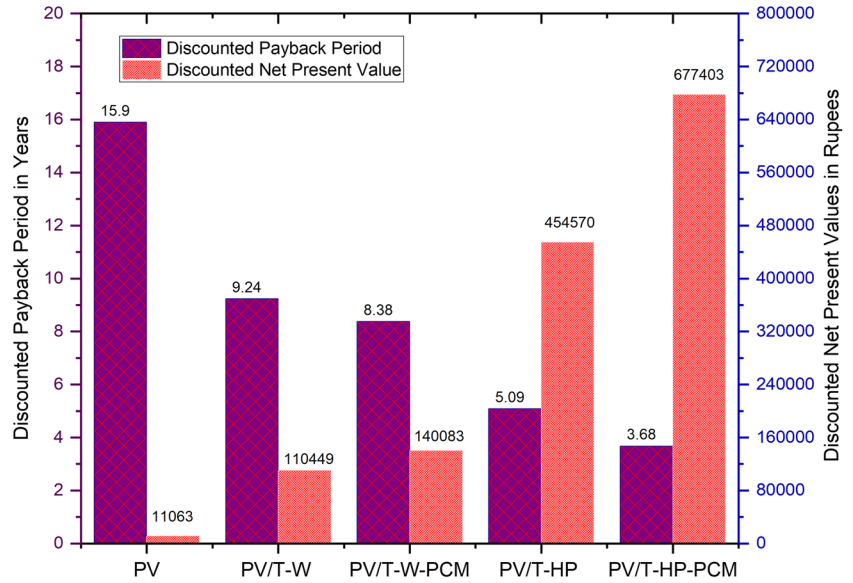


Fig. 13 Annual cash flow diagram of all cases

Fig. 14 Comparison of DPB and DNPV for cases 1, 2, 3, 4, and 5



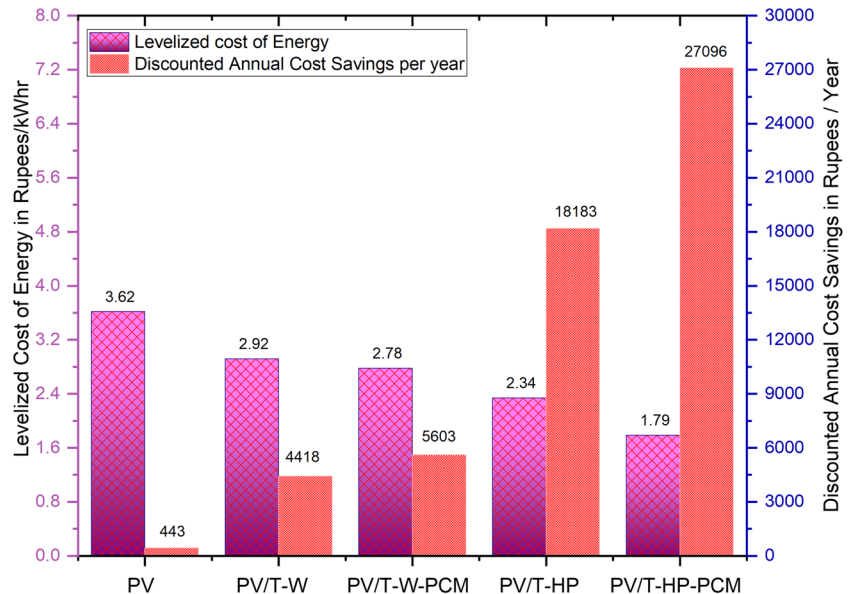
It can be inferred that the usage of case 1, 2, 3, and 4 systems effectively reduces CO₂, SO₂, NO_x, and PM₁₀ emissions, contributing to a reduced environmental impact. Therefore, the ecological and enviroeconomic cost analyses of case 1, 2, 3, and 4 systems are valid and demonstrate their worthiness. The results of the cost assessments reveal that the PV/T PCM-DXHP system is more affordable and preferable compared to the solar PV system and HVAC system working alone in the long term. As a result, more non-HVAC buildings should install solar PV/T PCM-W systems, and HVAC-system-integrated buildings should install PV/T PCM-DXHP systems to benefit from the economic rewards and enjoy a pristine environment for the foreseeable future.

Conclusion

Energy, economic, and environmental numerical analyses were carried out on PV/T-W, PV/T PCM-W, PV/T DXHP, and PV/T PCM-DXHP systems with a butterfly serpentine flow profile and HS36 PCM. The following is a summary of the most critical conclusions from the evaluation:

Energy performance: The average yearly electrical efficiencies of PV/T-W, PV/T PCM-W, PV/TDXHP, and PV/T PCM-DXHP systems are 9.77%, 10.57%, 11.83%, and 12.91%, which are 16.03%, 25.53%, 40.5%, and 53.32% higher than the reference PV system. The PV/T-W, PV/T PCM-W, PV/T DXHP, and PV/T PCM-

Fig. 15 Comparison of DACS and LCOE for cases 1, 2, 3, 4, and 5



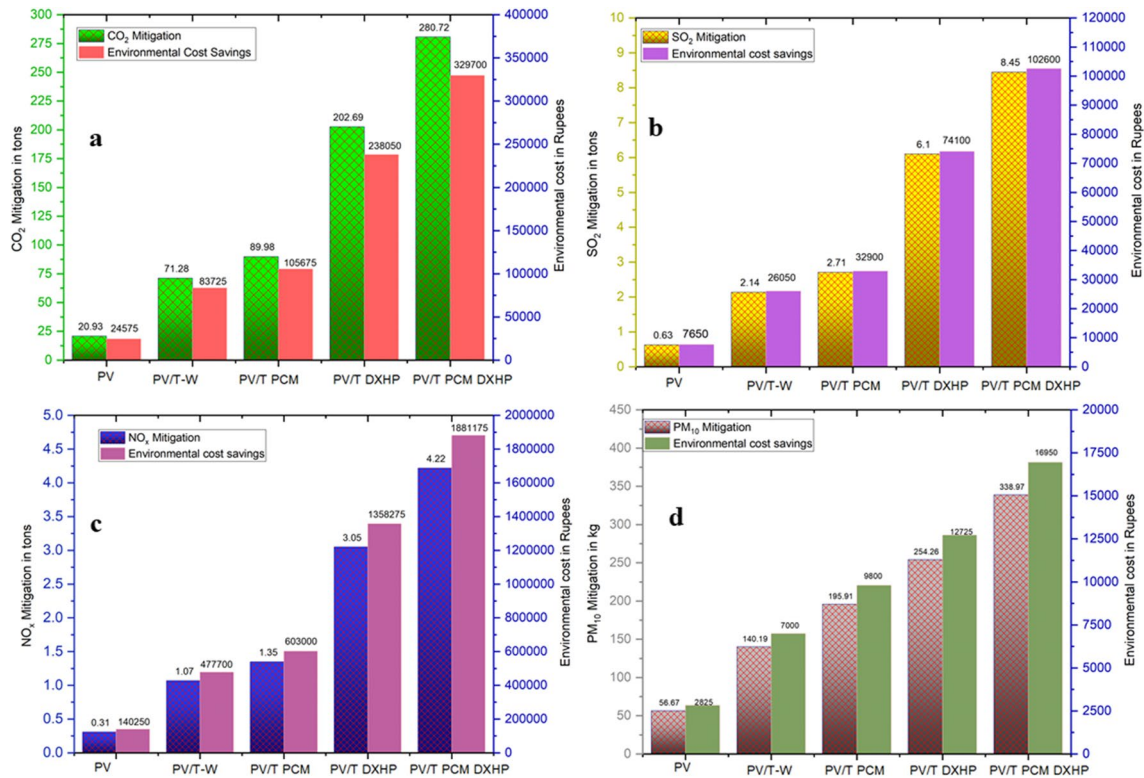


Fig. 16 Emission reduction and Environmental cost savings by cases 1, 2, 3, and 4: **a** CO₂, **b** SO₂, **c** NO_x, and **d** PM₁₀

DXHP systems produced 5709.35 MJ, 6801.16 MJ, 12,299.18 MJ, and 13,638.24 MJ, respectively. All the four systems with a BSF collector and HS36 PCM demonstrated improved energy performance. These systems produced higher electrical and thermal energy than the reference PV system. Notably, the PV/T PCM-DXHP system exhibited the highest energy production due to the integration of PCM and refrigerant for cooling.

Economic viability: The economic analysis showed a good result based on a discounted payback period of 8, 7, 6, and 5 years and the costs of energy production are ₹4.08 per kW-h, ₹3.67 per kW-h, ₹3.37 per kW-h, and ₹2.87 per kW-h for PV/T-W, PV/T PCM-W, PV/T DXHP, and PV/T PCM-DXHP systems, respectively. The financial analyses indicated that all four systems are economically viable. These systems' discounted net present values (DNPV) and discounted annual cost savings (DACs) were favorable, suggesting long-term profitability. Additionally, the payback periods for these systems were shorter than the reference PV system, further indicating their economic feasibility.

Environmental impact: The environmental analysis also showed a good result, and the proposed four systems mitigated the CO₂ of 64.72 tons, 90.45 tons, 117.35 tons, and 156.49 tons throughout their lifetimes. It saved the cost by ₹75,075, ₹104,925, ₹136,175, and ₹181,525. The PV/T-

W, PV/T PCM-W, PV/T DXHP, and PV/T PCM-DXHP systems demonstrated significant reductions in greenhouse gas emissions and other pollutants compared to the reference PV system. These systems contributed to the mitigation of carbon dioxide (CO₂), sulfur dioxide (SO₂), nitrogen oxides (NO_x), and PM₁₀ emissions. The magnitude of emissions reduction and cost savings varied among the different systems, with the PV/T PCM-DXHP system yielding the highest environmental benefits.

In conclusion, all the four systems with a butterfly serpentine flow profile and HS36 PCM demonstrated enhanced energy performance, economic viability, and environmental benefits. The findings support the feasibility and effectiveness of these systems for sustainable energy generation and environmental mitigation.

It is beneficial for the HVAC buildings to use the PV/T PCM-DXHP system, which can last up to at least 5 years because the results of the cost assessments reveal that the PV/T PCM -DXHP system is more affordable and more acceptable than the solar PV system and HVAC system working alone in the long term.

Subsequently, more non-HVAC buildings should install solar PV/T PCM-W systems and HVAC-system-integrated buildings should install PV/T PCM-DXHP systems to benefit from the economic rewards and relish in a pristine environment for the foreseeable future.

Nomenclature

DC: Direct current; *dg*: Module degradation; *Dr*: No. of days; *PVGC*: PV glassing cover; *SC*: Solar cell; *SSC*: Short circuit current; *FF*: Fill factor; *EVAN*: EVA grease; *EL*: Electrical insulation; *OD*: Outer diameter; *ID*: Inner diameter

Symbols

β : PV system slope ($^{\circ}$); *A*: PV area (m^2); *C*: Cost; *CF*: Cash flow; *G*: Solar irradiation (W/m^2); *m*: Mass (kg); *P*: Power (W); *p*: Pressure (bar); η : Efficiency (%); *P*: Electrical power (W); ΔP : Change in power (W); *Q*: Heat (kJ); *w*: Speed of the compressor; *T*: Temperature ($^{\circ}C$); \dot{m}_{ref} : The mass flow rate of refrigerants; *E*: Net energy (kWh/year); *i*: Inflation rate; *r*: Discount rate; ϕ : Mitigation per annum; ϕ : Emissions equivalents intensity for coal-fired electricity generation; *h'*: Enthalpy; *h*: Heat transfer coefficient; *U*: Overall heat transfer coefficient; *cl*: Collector; *d*: Conduction; *v*: Convection; *r'*: Radiation; *u*: Velocity; *V*: Displacement volume; *C_p*: Specific heat; ρ : Density; *L*: Length; α : Absorption coefficient; δ : Thickness; τ : Transmissivity; *g*: Glass; *abs*: Absorber

Symbols (subscript)

a: Ambient; *c*: Cell; *com*: Compressor; *con*: Condenser; *Eva*: Evaporator; *e*: Effectiveness; *exp*: Experimental; *El*: Electrical; *h*: Enthalpy; *iso*: Isometric; *in*: Inlet; *max*: Maximum; *min*: Minimum; *n*: Yearly; *o*: Initial Investment; *out*: Outlet; *O&M*: Operation and maintenance; *S*: Entropy; *S*: Sun; *S/Z*: Cost savings; *sim*: Simulation; *th*: Thermal; *t*: Year (no. of days); *tL*: Lifetime of components; *u*: Useful; *w*: Water; *X*: Readings; *Y*: Carbon price per ton

Acknowledgements The authors would like to mention their heartfelt gratitude and appreciation to the management of Bananri Amman Institute of Technology, India, for generously providing the necessary facilities and invaluable support to this research.

Author contribution All authors contributed to the study's conception and design. Methodology, material preparation, and data collection were performed by Prakash K. Babu and Amarkarthik Aruanchalam. Data collection and analysis were performed by Prakash K. Babu, Subramaniyan Chinnasamy, and Chandrasekaran Manimuthu. The first original draft of the manuscript was written by Prakash K. Babu and Subramaniyan Chinnasamy, and all authors commented on previous versions of the manuscript. All authors read and approved the final manuscript.

Data availability The article contains the data that was utilised to support the findings of this investigation. Additional data can be provided upon request.

Declarations

Ethical approval Not applicable.

Consent to participate Not applicable.

Consent for publication Not applicable.

Conflict of interest The authors declare no competing interests.

References

- Abbas S, Zhou J, Hassan A et al (2023) Economic evaluation and annual performance analysis of a novel series-coupled PV/T and solar TC with solar direct expansion heat pump system: An experimental and numerical study. *Renew Energy* 204:400–420. <https://doi.org/10.1016/j.renene.2023.01.032>
- Abdul Jabbar MH, Srivastava R, Abdul Manaf N et al (2023) The solar end game: bibliometric analysis, research and development evolution, and patent activity of hybrid photovoltaic/thermal—phase change material. *Environ Sci Pollut Res*. <https://doi.org/10.1007/s11356-023-27641-7>
- Alharbi FH, Kais S (2015) Theoretical limits of photovoltaics efficiency and possible improvements by intuitive approaches learned from photosynthesis and quantum coherence. *Renew Sustain Energy Rev* 43:1073–1089. <https://doi.org/10.1016/j.rser.2014.11.101>
- Amoatey P, Omidvarborna H, Baawain MS, Al-Mamun A (2019) Emissions and exposure assessments of SOX, NOX, PM10/2.5 and trace metals from oil industries: a review study (2000–2018). *Process Saf Environ Prot* 123:215–228. <https://doi.org/10.1016/j.psep.2019.01.014>
- Batool K, Zhao Z-Y, Irfan M et al (2023) Assessing the competitiveness of Indian solar power industry using the extended five forces model: a green innovation perspective. *Environ Sci Pollut Res* 30:82045–82067. <https://doi.org/10.1007/s11356-023-28140-5>
- Beniwal R, Kalra S, Singh Beniwal N, Gupta HO (2023) Smart photovoltaic system for Indian smart cities: a cost analysis. *Environ Sci Pollut Res* 30:45445–45454. <https://doi.org/10.1007/s11356-023-25600-w>
- Bhandari SB (2009) Discounted payback period—some extensions. *J Bus Behav Sci* 21(1):28–38
- Bhanja R, Roychowdhury K (2023) A spatial analysis of techno-economic feasibility of solar cities of India using Electricity System Sustainability Index. *Appl Geogr* 154:102893. <https://doi.org/10.1016/j.apgeog.2023.102893>
- Bianchini A, Guzzini A, Pellegrini M, Saccani C (2017) Photovoltaic/thermal (PV/T) solar system: experimental measurements, performance analysis and economic assessment. *Renew Energy* 111:543–555. <https://doi.org/10.1016/j.renene.2017.04.051>
- Caliskan H, Dincer I, Hepbasli A (2012) Exergoeconomic, environmental and sustainability analyses of a novel air cooler. *Energy Build* 55:747–756. <https://doi.org/10.1016/j.enbuild.2012.03.024>
- Canelli M, Entchev E, Sasso M et al (2015) Dynamic simulations of hybrid energy systems in load sharing application. *Appl Therm Eng* 78:315–325. <https://doi.org/10.1016/j.applthermaleng.2014.12.061>
- Coffey B, McLaughlin PA, Peretto PF (2016) The cumulative cost of regulations. *SSRN Electron J*. <https://doi.org/10.2139/ssrn.2869145>
- Cui Y, Zhu J, Zhang F et al (2022) Current status and future development of hybrid PV/T system with PCM module: 4E (energy, exergy, economic and environmental) assessments. *Renew Sustain Energy Rev* 158:112147. <https://doi.org/10.1016/j.rser.2022.112147>
- Dannemand M, Perers B, Furbo S (2019) Performance of a demonstration solar PVT assisted heat pump system with cold buffer storage and domestic hot water storage tanks. *Energy Build* 188–189:46–57. <https://doi.org/10.1016/j.enbuild.2018.12.042>
- Dannemand M, Sifnaios I, Tian Z, Furbo S (2020) Simulation and optimization of a hybrid unglazed solar photovoltaic-thermal collector and heat pump system with two storage tanks. *Energy Convers Manag* 206:112429. <https://doi.org/10.1016/j.enconman.2019.112429>

- den Elzen MGJ, Hof AF, Mendoza Beltran A et al (2011) The Copenhagen Accord: abatement costs and carbon prices resulting from the submissions. *Environ Sci Policy* 14:28–39. <https://doi.org/10.1016/j.envsci.2010.10.010>
- Deng W, Yu J (2016) Simulation analysis on dynamic performance of a combined solar/air dual source heat pump water heater. *Energy Convers Manag* 120:378–387. <https://doi.org/10.1016/j.enconman.2016.04.102>
- Dubey S, Sarvaiya JN, Seshadri B (2013) Temperature Dependent photovoltaic (PV) efficiency and its effect on PV production in the world – a review. *Energy Procedia* 33:311–321. <https://doi.org/10.1016/j.egypro.2013.05.072>
- Ehyaie MA, Ahmadi A, Rosen MA (2019) Energy, exergy, economic and advanced and extended exergy analyses of a wind turbine. *Energy Convers Manag* 183:369–381. <https://doi.org/10.1016/j.enconman.2019.01.008>
- Emmanuel B, Yuan Y, Maxime B et al (2021) A review on the influence of the components on the performance of PVT modules. *Sol Energy* 226:365–388. <https://doi.org/10.1016/j.solener.2021.08.042>
- Fawzy S, Osman AI, Doran J, Rooney DW (2020) Strategies for mitigation of climate change: a review. *Environ Chem Lett* 18:2069–2094. <https://doi.org/10.1007/s10311-020-01059-w>
- Gielen D, Boshell F, Saygin D et al (2019) The role of renewable energy in the global energy transformation. *Energy Strateg Rev* 24:38–50. <https://doi.org/10.1016/j.esr.2019.01.006>
- Gu Y, Zhang X, Are Myhren J et al (2018) Techno-economic analysis of a solar photovoltaic/thermal (PV/T) concentrator for building application in Sweden using Monte Carlo method. *Energy Convers Manag* 165:8–24. <https://doi.org/10.1016/j.enconman.2018.03.043>
- Guarracino I, Mellor A, Ekins-Daukes NJ, Markides CN (2016) Dynamic coupled thermal-and-electrical modelling of sheet-and-tube hybrid photovoltaic/thermal (PVT) collectors. *Appl Therm Eng* 101:778–795. <https://doi.org/10.1016/j.applthermaleng.2016.02.056>
- Guo C, Ji J, Sun W et al (2015) Numerical simulation and experimental validation of tri-functional photovoltaic/thermal solar collector. *Energy* 87:470–480. <https://doi.org/10.1016/j.energy.2015.05.017>
- Herbohn JL, Harrison SR (2002) Introduction to discounted cash flow analysis and financial functions in excel. *Socio-Economic Research Methods in Forestry: A Training Manual*, Leyte State University, ViSCA, Baybay
- Herrando M, Markides CN (2016) Hybrid PV and solar-thermal systems for domestic heat and power provision in the UK: techno-economic considerations. *Appl Energy* 161:512–532. <https://doi.org/10.1016/j.apenergy.2015.09.025>
- Hossain MS, Pandey AK, Selvaraj J et al (2019) Two side serpentine flow based photovoltaic-thermal-phase change materials (PVT-PCM) system: energy, exergy and economic analysis. *Renew Energy* 136:1320–1336. <https://doi.org/10.1016/j.renene.2018.10.097>
- Jäger-Waldau A, Kougias I, Taylor N, Thiel C (2020) How photovoltaics can contribute to GHG emission reductions of 55% in the EU by 2030. *Renew Sustain Energy Rev* 126:109836. <https://doi.org/10.1016/j.rser.2020.109836>
- Kaleshwarwar A, Bahadure S (2023) Assessment of the solar energy potential of diverse urban built forms in Nagpur, India. *Sustain Cities Soc* 96:104681. <https://doi.org/10.1016/j.scs.2023.104681>
- Kalogirou SA, Tripanagnostopoulos Y (2007) Industrial application of PV/T solar energy systems. *Appl Therm Eng* 27:1259–1270. <https://doi.org/10.1016/j.applthermaleng.2006.11.003>
- Kazem HA, Al-Waeli AHA, Chaichan MT, Alnaser WE (2023) Photovoltaic/thermal systems for carbon dioxide mitigation applications: a review. *Front Built Environ* 9. <https://doi.org/10.3389/fbuil.2023.1211131>
- Lamba R, Montero FJ, Rehman T et al (2023) PCM-based hybrid thermal management system for photovoltaic modules: a comparative analysis. *Environ Sci Pollut Res*. <https://doi.org/10.1007/s11356-023-27809-1>
- Liu Y, Zhang H, Chen H (2020) Experimental study of an indirect-expansion heat pump system based on solar low-concentrating photovoltaic/thermal collectors. *Renew Energy* 157:718–730. <https://doi.org/10.1016/j.renene.2020.05.090>
- Liu W, Yao J, Jia T et al (2023) The performance optimization of DX-PVT heat pump system for residential heating. *Renew Energy* 206:1106–1119. <https://doi.org/10.1016/j.renene.2023.02.089>
- Lu S, Liang R, Zhang J, Zhou C (2019) Performance improvement of solar photovoltaic/thermal heat pump system in winter by employing vapor injection cycle. *Appl Therm Eng* 155:135–146. <https://doi.org/10.1016/j.applthermaleng.2019.03.038>
- Miglioli A, Aste N, Del Pero C, Leonforte F (2021) Photovoltaic-thermal solar-assisted heat pump systems for building applications: integration and design methods. *Energy Built Environ*. <https://doi.org/10.1016/j.enbenv.2021.07.002>
- Muthu V, Ramadas G (2023) Performance studies of Bifacial solar photovoltaic module installed at different orientations: energy, exergy, enviroeconomic, and exergo-enviroeconomic analysis. *Environ Sci Pollut Res* 30:62704–62715. <https://doi.org/10.1007/s11356-023-26406-6>
- Obalanlege MA, Mahmoudi Y, Douglas R et al (2020) Performance assessment of a hybrid photovoltaic-thermal and heat pump system for solar heating and electricity. *Renew Energy* 148:558–572. <https://doi.org/10.1016/j.renene.2019.10.061>
- Obalanlege MA, Xu J, Markides CN, Mahmoudi Y (2022) Techno-economic analysis of a hybrid photovoltaic-thermal solar-assisted heat pump system for domestic hot water and power generation. *Renew Energy* 196:720–736. <https://doi.org/10.1016/j.renene.2022.07.044>
- Poredoš P, Tomc U, Petelin N et al (2020) Numerical and experimental investigation of the energy and exergy performance of solar thermal, photovoltaic and photovoltaic-thermal modules based on roll-bond heat exchangers. *Energy Convers Manag* 210:112674. <https://doi.org/10.1016/j.enconman.2020.112674>
- Prakash KB, Amarkarthik A (2023) Energy analysis of a novel butterfly serpentine flow-based PV/T and PV/T heat pump system with phase change material – an experimental comparative study. *Energy Sources, Part A Recover Util Environ Eff* 45:5494–5507. <https://doi.org/10.1080/15567036.2023.2209526>
- Rajoria CS, Agrawal S, Tiwari GN (2013) Exergetic and enviroeconomic analysis of novel hybrid PVT array. *Sol Energy* 88:110–119. <https://doi.org/10.1016/j.solener.2012.11.018>
- Rappaport A (1965) Discounted payback period. *Management Services: A Magazine of Planning, Systems, and Controls* 2(4):Article 4
- Rauf A, Nureen N, Irfan M, Ali M (2023) The current developments and future prospects of solar photovoltaic industry in an emerging economy of India. *Environ Sci Pollut Res* 30:46270–46281. <https://doi.org/10.1007/s11356-023-25471-1>
- Sharaf M, Yousef MS, Huzayyin AS (2022) Review of cooling techniques used to enhance the efficiency of photovoltaic power systems. *Environ Sci Pollut Res* 29:26131–26159. <https://doi.org/10.1007/s11356-022-18719-9>
- Tiwari GN, Yadav JK, Singh DB et al (2015) Exergoeconomic and enviroeconomic analyses of partially covered photovoltaic flat plate collector active solar distillation system. *Desalination* 367:186–196. <https://doi.org/10.1016/j.desal.2015.04.010>
- Tse K-K, Chow T-T, Su Y (2016) Performance evaluation and economic analysis of a full scale water-based photovoltaic/thermal (PV/T) system in an office building. *Energy Build* 122:42–52. <https://doi.org/10.1016/j.enbuild.2016.04.014>

- Velmurugan K, Kumarasamy S, Wongwuttanasatian T, Seithanabutara V (2021) Review of PCM types and suggestions for an applicable cascaded PCM for passive PV module cooling under tropical climate conditions. *J Clean Prod* 293:126065. <https://doi.org/10.1016/j.jclepro.2021.126065>
- Waqas A, Jie J (2018) Effectiveness of phase change material for cooling of photovoltaic panel for hot climate. *J Sol Energy Eng* 140. <https://doi.org/10.1115/1.4039550>
- Yang, Zhou, Yuan (2019) Energy performance of an encapsulated phase change material PV/T system. *Energies* 12:3929. <https://doi.org/10.3390/en12203929>
- Zhang X, Shen J, Xu P et al (2014) Socio-economic performance of a novel solar photovoltaic/loop-heat-pipe heat pump water heating system in three different climatic regions. *Appl Energy* 135:20–34. <https://doi.org/10.1016/j.apenergy.2014.08.074>
- Zhou C, Liang R, Zhang J, Riaz A (2019) Experimental study on the cogeneration performance of roll-bond-PVT heat pump system with single stage compression during summer. *Appl Therm Eng* 149:249–261. <https://doi.org/10.1016/j.applthermaleng.2018.11.120>

Publisher's Note Springer Nature remains neutral with regard to jurisdictional claims in published maps and institutional affiliations.

Springer Nature or its licensor (e.g. a society or other partner) holds exclusive rights to this article under a publishing agreement with the author(s) or other rightsholder(s); author self-archiving of the accepted manuscript version of this article is solely governed by the terms of such publishing agreement and applicable law.